

Figure S11. Geographical distribution of the time when T_{\max} appears (in UTC hour) and the corresponding differences from the time when PBL_{\max} and SH_{\max} occur. The plots are derived from the 3-hourly ERA-Interim reanalysis.

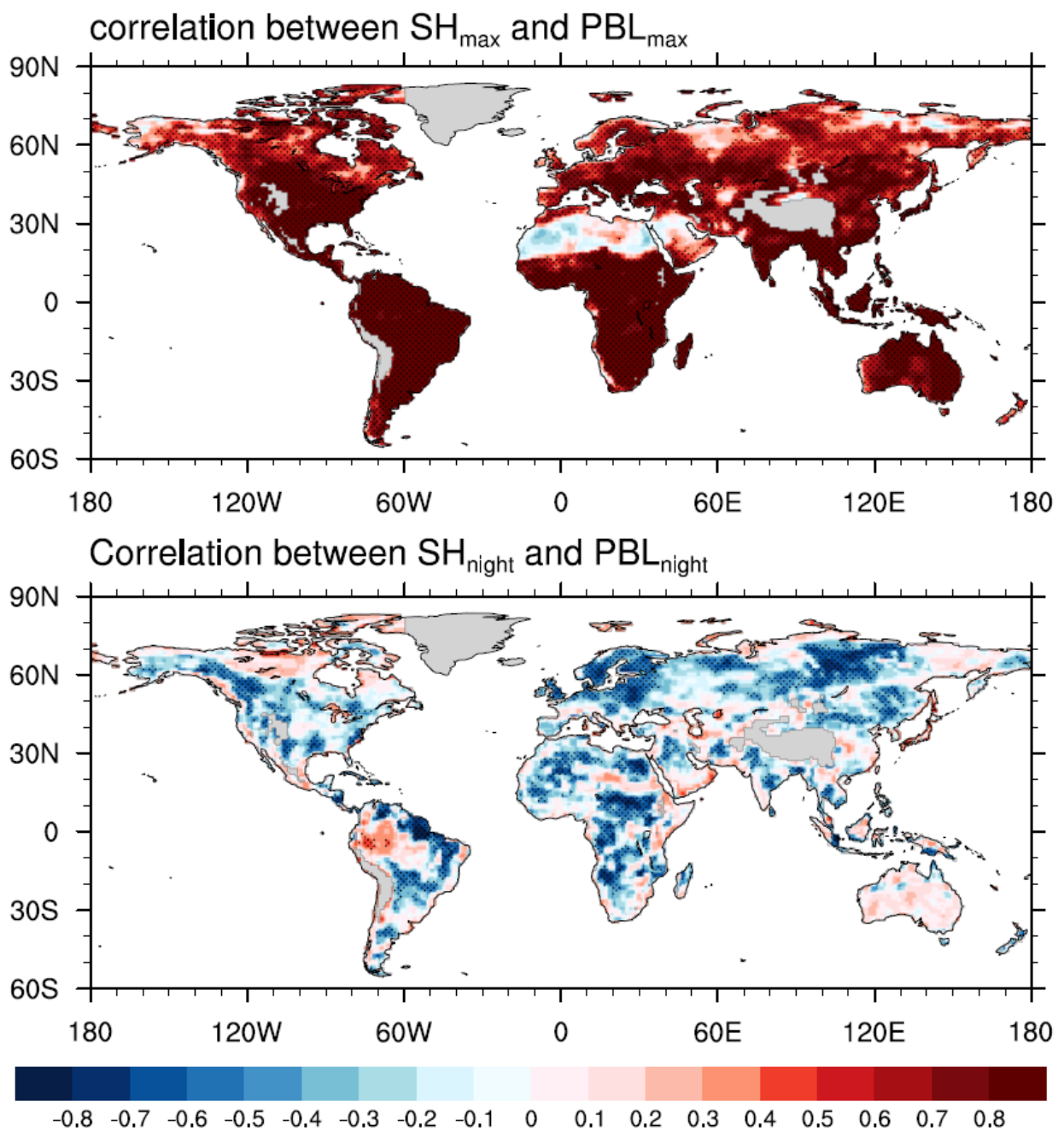


Figure SI2. Geographical distribution of the inter-annual correlations between SH_{\max} and PBL_{\max} (top panel), and between SH_{night} and PBL_{night} (bottom panel) from the ERA-Interim reanalysis

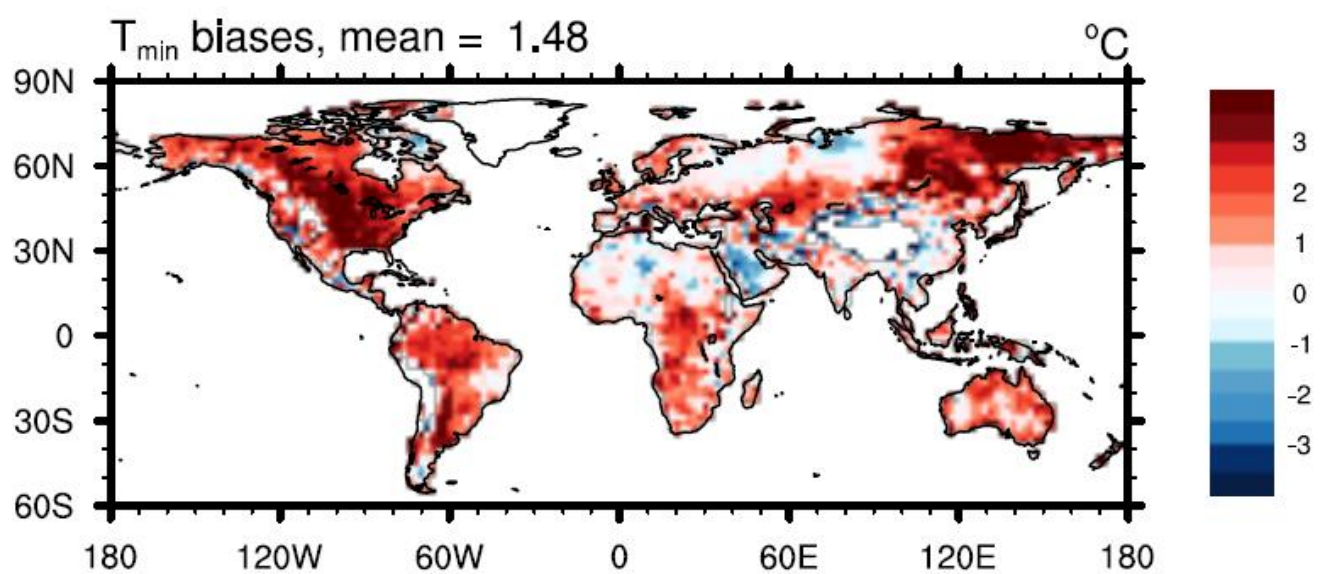
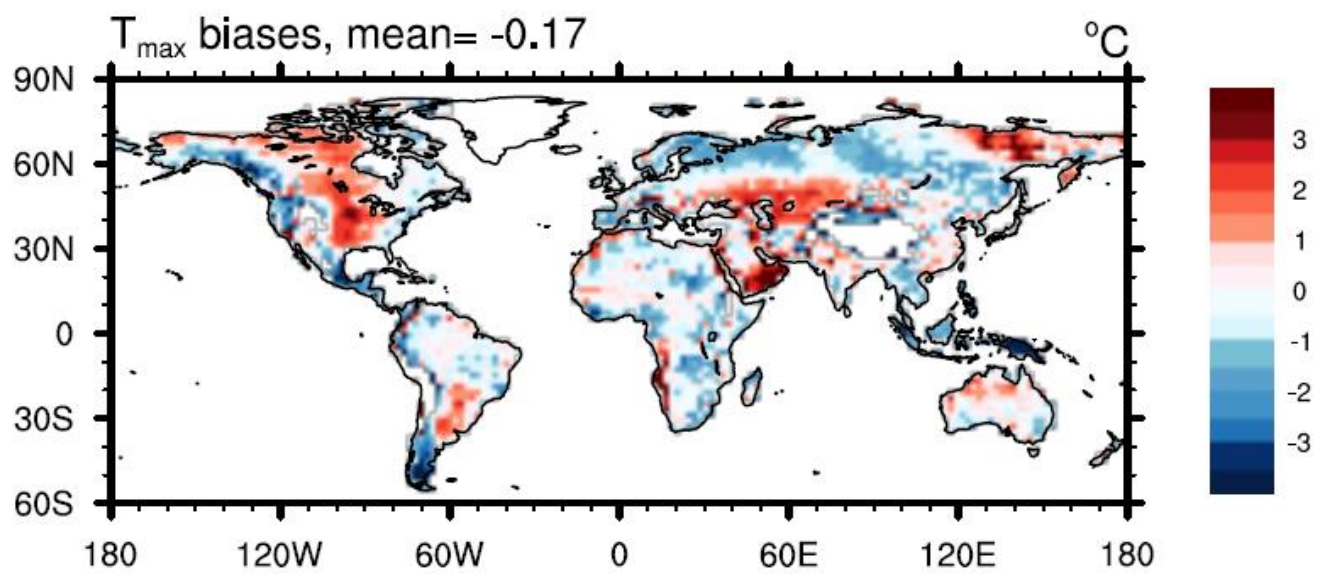
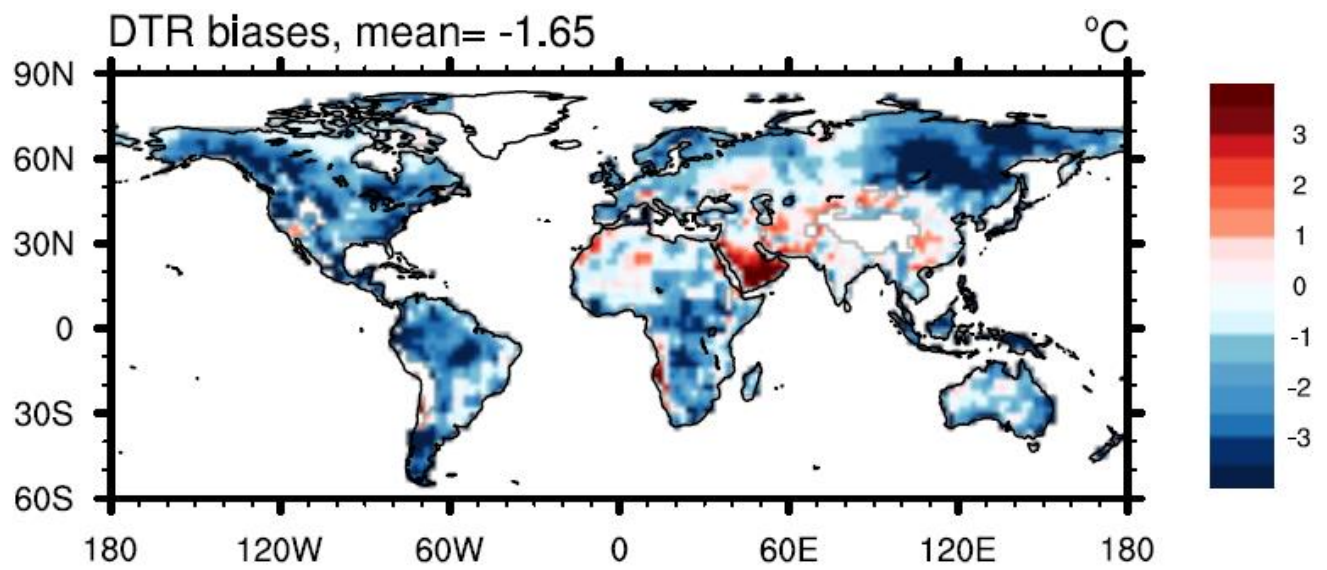


Figure SI3. Geographical distribution of the CFMIP2-simulated multi-model ensemble mean biases of DTR, T_{\max} and T_{\min} ($^{\circ}\text{C}$) against the CRU observations

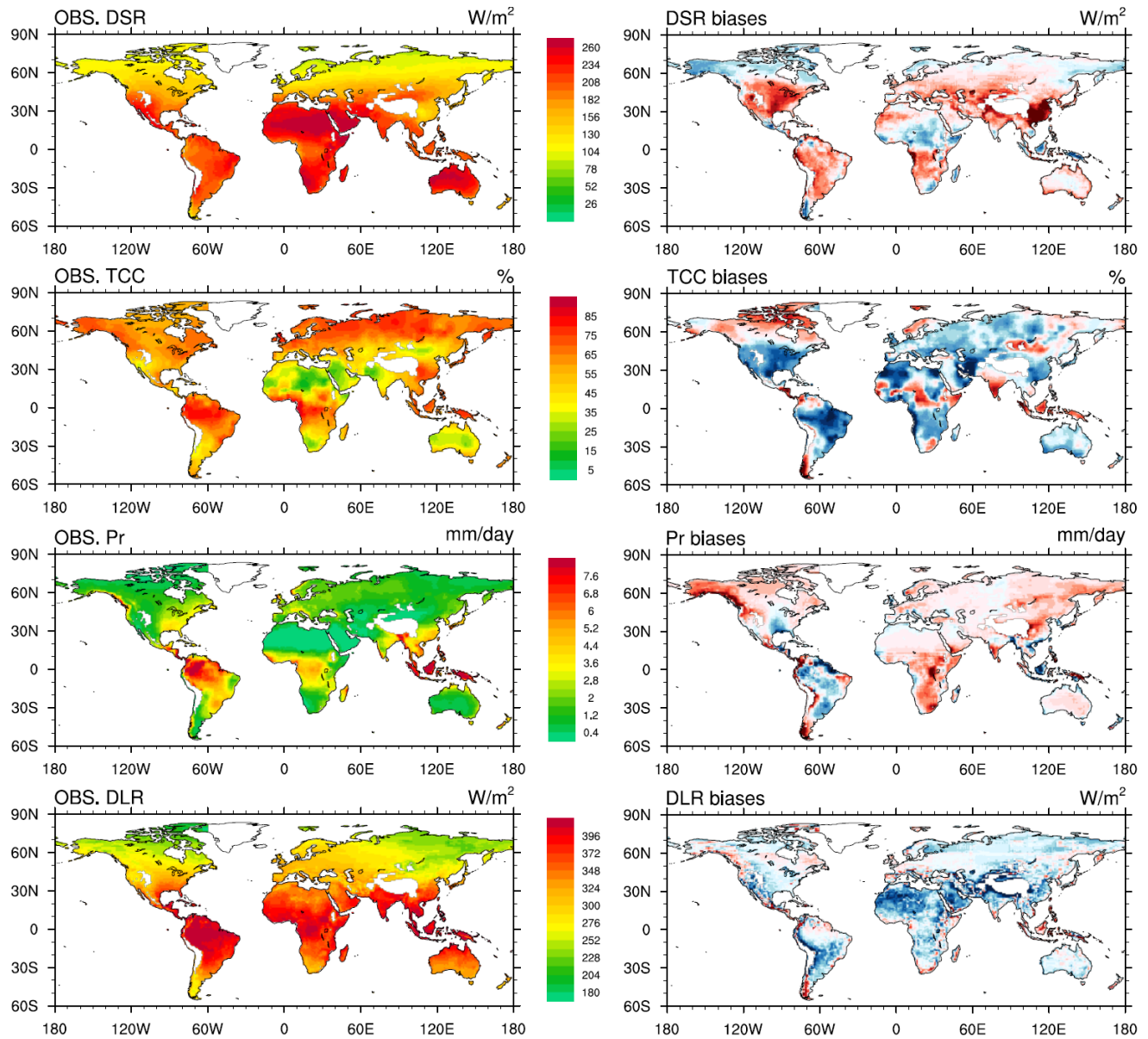


Figure SI4. Geographical distribution of (left panels) the observed climatological downward shortwave radiation (DSR, W/m^2) from the CERES-EBAF data, total cloud cover (TCC, %) from the CRU data, precipitation (Pr, mm/day) from the GPCP data, and downward longwave radiation (DLR, W/m^2) from the CERES-EBAF data, and (right panels) the corresponding CMIP5 multi-model ensemble mean biases